Brownian dynamics simulation of dense binary colloidal mixtures: II. Translational and bond-orientational order

Subrata Sanyal* and Ajay K. Sood†
Department of Physics, Indian Institute of Science, Bangalore 560 012, India
(Received 21 February 1995)

We report the Brownian dynamics simulation results on the translational and bond-angle-orientational correlations for charged colloidal binary suspensions as the interparticle interactions are increased to form a crystalline (for a volume fraction $\phi = 0.2$) or a glassy ($\phi = 0.3$) state. The translational order is quantified in terms of the two- and four-point density autocorrelation functions whose comparisons show that there is no growing correlation length near the glass transition. The nearest-neighbor orientational order is determined in terms of the quadratic rotational invariant Q_l and the bond-orientational correlation functions $g_l(t)$. The l dependence of Q_l indicates that icosahedral ($l = 6$) order predominates at the cost of the cubic order ($l = 4$) near the glass as well as the crystal transition. The density and orientational correlation functions for a supercooled liquid freezing towards a glass fit well to the stretched-exponential form $\exp[-(t/\tau)^\beta]$. The average relaxation times extracted from the fitted stretched-exponential functions as a function of effective temperatures T^* obey the Arrhenius law for liquids freezing to a crystal whereas these obey the Vogel-Tamman-Fulcher law $\exp[AT_0^*/(T^* - T_0^*)]$ for supercooled liquids tending towards a glassy state. The value of the parameter A suggests that the colloidal suspensions are "fragile" glass formers like the organic and molecular liquids.

PACS number(s): 82.70.Dd, 61.20.Ja, 05.40.+j, 64.70.Dv

I. INTRODUCTION

The nature of translational and bond-orientational orders [1] in liquids as a function of temperature has been studied in the past few years and is still to be understood completely. The motivation to look for these orders in three-dimensional systems [2] has come from the observation of the "hexatic" phase in two dimensions with sixfold bond-orientational order but no translational order. A suitable order parameter to investigate the bond-orientational order, called the quadratic rotational invariant Q_l (defined below), was introduced in the pioneering work of Steinhardt *et al.* [3]. Their molecular dynamics (MD) simulations of one-component Lennard-Jones (LJ) system [3] have shown the presence of extended bond-orientational order (predominantly icosahedral) but short-range translation order in a supercooled liquid. One of the rationale of this observation was the original idea of Frank [4] that icosahedral clusters are lower-energy configurations than other microcrystalline arrangements. In subsequent papers, Nelson and Widom [5] had shown that frustration effects prevent the existence of infinite-range icosahedral ordering. The concept of icosahedral ordering has been frequently used to model dynamics in supercooled liquids and glasses [6]. The order parameter Q_l and the associated correlation function $\psi_l(t) = \langle Q_l(0)Q_l(t)\rangle$ have been used quite extensively as important tools in computer simulations not only to quantify icosahedral order in monodisperse or binary supercooled liquids [7–11] but also to study crystal nucleation [11,12]. Other techniques [13–15] have also been suggested to quantify the icosahedral order. We note that some studies [11,13], contrary to the above results, have failed to show predominant icosahedral order in the supercooled liquid states. In a recent paper, Clarke and Jónsson [15] have studied the effect of densification on random hard-sphere packing and shown that the icosahedral ordering can arise from packing constraints alone.

As a liquid is cooled, its characteristic time scale grows rapidly and finally diverges at the glass transition (GT). Associating this growth with an underlying thermodynamic phase transition with a correspondingly growing correlation length scale, similar to the spin-glass transition [16], is a central theme of many theoretical studies [17,18] of the GT. Even though a large number of experiments [19] and computer simulation [9,10] have failed to produce any indication of such a diverging length scale, recent experimental data [20] are still being interpreted in these terms, keeping the issue still controversial.

The interparticle interaction of the aqueous suspensions of charge-stabilized polystyrene spheres (polyballs) [21] can be easily tuned so that the suspensions can mimic structural and dynamic behavior similar to simple atomic fluids and solids. In this paper, we present the study of translational as well as orientational order of binary polyball mixtures while reducing its effective tempera-

*Present address: Department of Chemical and Nuclear Engineering, University of California at Santa Barbara, Santa Barbara, CA 93106. Electronic address: subrata@squid.ucsb.edu
†Also at Jawaharlal Nehru Centre for Advanced Scientific Research, Jakkur Campus, P.O. Jakkur, Bangalore 560 064, India. Electronic address: asood@physics.iisc.ernet.in

ture from a liquid to a crystal and also to a glass. The static properties and the mean-squared displacements of the same system are reported in the preceding paper (hereafter called paper I) [22]. These, together with other dynamic properties such as the van Hove correlation function [23] of these states, supplement our studies of translational and bond-orientational orders to arrive at some understanding of the cooperative behavior. The model and the simulation procedure are described in detail in paper I [22]. Section II of this paper is devoted to the results of our simulations and Sec. III contains the summary of our findings and conclusions of this work.

II. RESULTS

In this section we report the results of our Brownian dynamics (BD) simulation study of the translational as well as bond-orientational order parameters as a binary dense liquid is effectively "cooled" by reducing n_i in 12 steps to a crystal for $\phi = 0.2$ or to a glass for $\phi = 0.3$ [24–30]. The translational order has been quantified by the normalized two-point $c_2(t)$ and the four-point $C_4(r,t)$ density-correlation functions in Sec. II A. The Sec. II B provides details of the computations of the quadratic rotational invariant Q_l and the normalized bond-orientational autocorrelation functions $g_l(t)$ to quantify the bond-orientational order. The density and bond-orientational relaxation times, extracted from the stretched-exponential fits of the above correlation functions, are dealt with in Sec. II C.

A. Translational order

1. *Density autocorrelation function*

Following the work of Dasgupta *et al.* to evaluate the density correlation functions [9], we subdivide the system of $N = 432$ particles into a lattice of $M \times M \times M$ ($M = 10$) cubic cells with side a_s. Each cell is labeled by one of its vertices i or equivalently by $\vec{r}_i$ with respect to a reference coordinate frame fixed by the simulation box. One can then define a two-point density autocorrelation function as

$$C_2(t) = [\langle n(i,t_0)n(i,t_0+t)\rangle], \tag{1}$$

using a lattice-gas variable $n(i,t) = \mathrm{sgn}[m_i(t) - \bar{m}]$, where $m_i(t)$ is the number of particles at time t in the cell i and $\bar{m}$ is the average number of particles per cell. The angular and the square brackets throughout this paper indicate the averages over initial times t_0 and over sites i, respectively. Figure 1 shows the values of $m_0 = [\langle n(i,t)\rangle]$ as a function of $T^\star$ for the crystalline transition (CT) ($\phi = 0.2$) and the GT ($\phi = 0.3$). Since the total number of cubic cells (equal to 1000) here is greater than $2N$, m_0 is negative. If the centers of two particles get closer than the cell diagonal $\sqrt{3}a_s$, both of them contribute to the same cell. This is more likely at high temperatures where the underlying order is fluidlike, leaving empty cells more

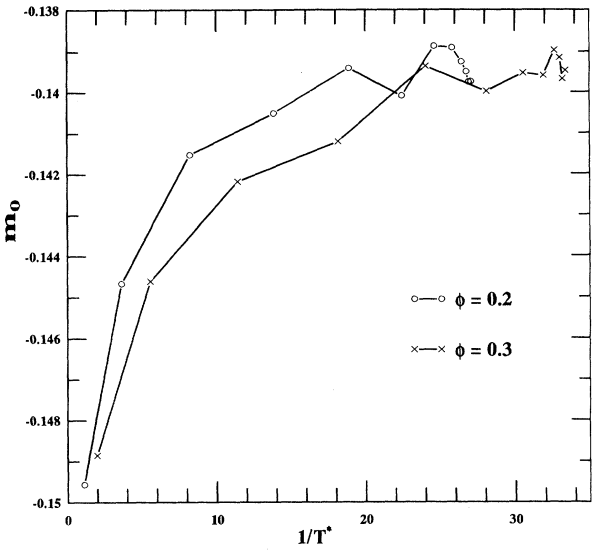

FIG. 1. Plot of $m_0 = [\langle n(i,t)\rangle]$ versus $1/T^\star$ for the liquid to crystal transition ($\phi = 0.2$) and the liquid to glass transition ($\phi = 0.3$).

than $M^3 - 2N$ and hence resulting in a decreased value of m_0 compared to that at low temperatures. We note that by definition $C_2(t=0) \equiv 1$ and that it asymptotically decays to $C_2(t \to \infty) = m_0^2$ in a fluid phase. To keep its value between 0 and 1 so that any asymptotic nonzero value of this correlation function signifies the arrested motion, characteristic of a solid (crystal or glass) state, we define a scaled (or normalized) density correlation function

$$c_2(t) = \frac{C_2(t) - m_0^2}{1 - m_0^2}. \tag{2}$$

Figures 2 and 3 show the growth of $c_2(t)$ as a function of time t at seven different runs for $\phi = 0.2$ and Figs. 4 and 5 show $c_2(t)$ for $\phi = 0.3$ at eight different runs. By comparing Fig. 2(c) with 2(d) and Fig. 5(a) with 5(c), we can clearly see that in each case, at lower temperatures the system is more mobile, i.e., the correlation function comparatively decays more. These results (see Fig. 6 also) indicate that freezing for both the crystal and the glass, in our system, is a "three-stage" process. There is a monotonic increase of the area under the curve $c_2(t)$ (i.e., the density relaxation time) with lowering the temperature until some particular value (say $T_1^\star$), below which the area decreases, indicating the surprising retrieval of a more liquidlike (mobile) state up to a second temperature $T_2^\star$ ($< T_1^\star$). Upon further cooling, the long-time tail of $c_2(t)$ increases in magnitude until the final ($n_i = 0$) crystalline ($\phi = 0.2$) or amorphous state ($\phi = 0.3$) is reached. The temperatures $T_1^\star$ and $T_2^\star$ are more precisely found out in a later subsection (II C) from the plot of the relaxation time, extracted from these correlation functions, as a function of $T^\star$. The evolution of the dynamics and the three-stage process, as apparent from these correlation functions, are perfectly consistent with the Einstein plots (mean-square displacement ver-

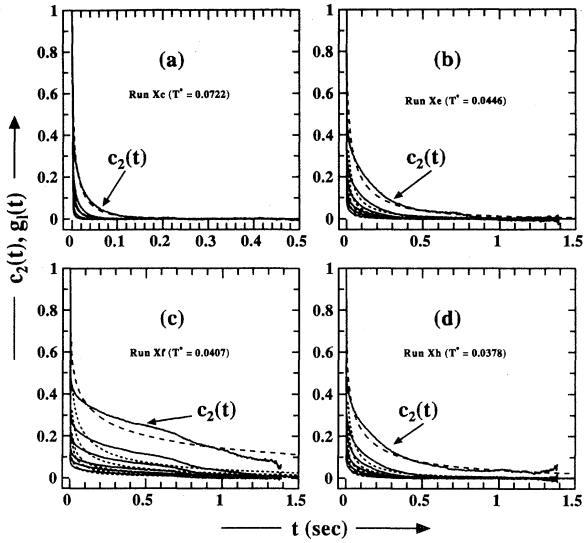

FIG. 2. Temporal growth of the normalized density autocorrelation $c_2(t)$ and the bond-orientational correlation $g_l(t)$ functions for $l = 2, 4, 6, 8, 10$ (solid lines) along with their stretched-exponential [Eq. (8)] fits (dashed lines) for the runs (a) Xc, (b) Xe, (c) Xf, and (d) Xh with $\phi = 0.2$. In (a), the fit is shown only for $c_2(t)$ to avoid overcrowding of curves. The sequence of curves from top to bottom in each panel is $c_2(t)$, $g_6(t)$, $g_4(t)$, $g_2(t)$, $g_8(t)$, and $g_{10}(t)$.

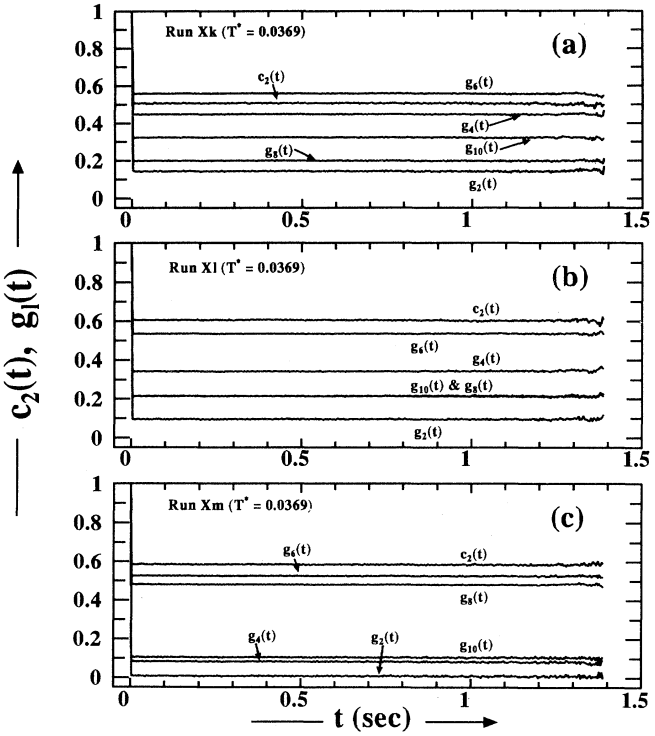

FIG. 3. Functions $c_2(t)$ and $g_l(t)$ for $l = 2, 4, 6, 8, 10$ for the runs (a) Xk, (b) Xl, and (c) Xm, all with $\phi = 0.2$ and $n_i = 0$. The sequence of curves from top to bottom is marked in the respective panels.

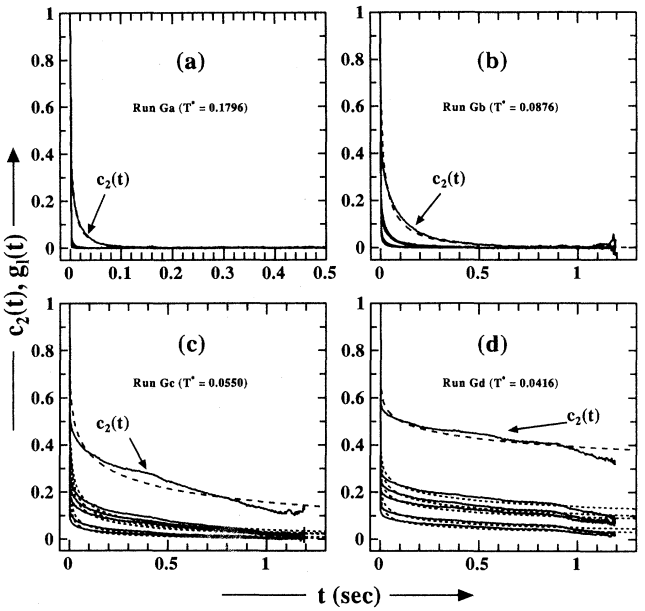

FIG. 4. Same as in Fig. 2 but for $\phi = 0.3$ and the runs (a) Ga, (b) Gb, (c) Gc, and (d) Gd. Fits to Eq. (8) for only $c_2(t)$ are shown in (a) and (b) to avoid overcrowding of data. The sequence of curves from top to bottom in each panel is $c_2(t)$, $g_6(t)$, $g_4(t)$, $g_2(t)$, $g_8(t)$, and $g_{10}(t)$.

sus time) in both cases, which are shown in paper I [22] and elsewhere [23,30]. Below $T_2^\star$, the respective CT or GT takes place, which arrests the particle motion to show long-time saturations in $c_2(t)$.

2. *Four-point density correlation function*

We have also computed more general space-time correlation functions defined by [9]

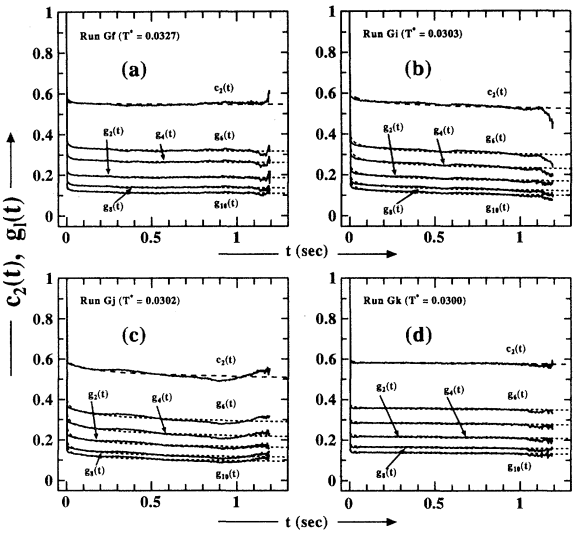

FIG. 5. Same as in Fig. 4 but for the runs (a) Gf, (b) Gi, (c) Gj, and (d) Gk, with $\phi = 0.3$. The sequence of curves from top to bottom are marked in the respective panels.

$$C_4(\vec{r},t) = [\langle n(\vec{r}_i,t_0)n(\vec{r}_i+\vec{r},t_0) \times n(\vec{r}_i,t_0+t)n(\vec{r}_i+\vec{r},t_0+t)\rangle] \quad (3)$$

and

$$C_4(\vec{r}) = [\langle n(\vec{r}_i,t_0)n(\vec{r}_i+\vec{r},t_0)\rangle^2] = \lim_{t\to\infty} C_4(\vec{r},t). \quad (4)$$

Figure 6 shows the plot of $C_4(r = 2.45a_s, t)$ by continuous lines and $[C_2(t)]^2$ by dashed lines for $\phi = 0.2$ in panel (a) and $\phi = 0.3$ in panel (b). We note that if the system has spatial correlations of range less than $\vec{r}$, then $C_4(\vec{r},t)$ should be identical to $[C_2(t)]^2$. As can be clearly seen from Fig. 6(a), the difference between the two functions increases with reducing the temperature for the CT. By contrast, we see from Fig. 6(b) that $C_4(\vec{r},t) \equiv [C_2(t)]^2$, implying that any correlation present in the system decays in less than $r \sim 2.5a_s$. This points to the absence of any diverging correlation length near the GT, in agreement with the previous simulations [9,10] and experiments [19]. It not only contradicts the idea of identifying the GT as a thermodynamic phase transition associated with a corresponding divergent length scale [17] but also rules out the possibility of the spatial growth of the noncrystallographic clumps of particles ("amorphons") near the GT, as speculated by Hoare [31].

B. Bond-orientational order

The nearest-neighbor orientational order in computer simulations can be calculated by quadratic rotational invariants [3] and bond-orientational autocorrelation functions [9]. The simulation box is meshed into $M \times M \times M$ cubic cells as before. We consider each pair of nearest neighbors, lying at a distance less than the first minimum of its partial pair distribution functions (PDF's), to be interconnected by lines ("bonds"). With respect to the coordinate system fixed by the box, if $(\theta_\alpha, \phi_\alpha)$ is the orientation of a bond α, then depending on the proximity of the bond center $\vec{r}_\alpha$ to one of the eight vertices i (i.e., $\vec{d}_{i\alpha} = \vec{r}_\alpha - \vec{r}_i$), we define a weight function [9]

$$w_\alpha^i = \frac{\exp[-(d_{i\alpha}/a_s)]}{\sum_j \exp[-(d_{j\alpha}/a_s)]} \quad (5)$$

and orientational order parameters $Q_{lm}(\vec{r}_\alpha,t) = Y_{lm}(\theta_\alpha(t),\phi_\alpha(t))$, where $\{Y_{lm}\}$ are the spherical harmonics. We evaluate the quadratic rotational invariant

$$Q_l = \left[\frac{4\pi}{2l+1}\sum_{m=-l}^{l}\left\langle\left|\frac{1}{N_{\text{bonds}}}\sum_{\alpha=1}^{N_{\text{bonds}}} Q_{lm}(\vec{r}_\alpha,t)\right|^2\right\rangle\right]^{1/2} \quad (6)$$

and the temporal evolution of the bond-orientational autocorrelation function

$$G_l(t) = \frac{4\pi}{2l+1}\sum_{m=-l}^{l}[\langle W_{lm}(i,t_0)W_{lm}^\star(i,t_0+t)\rangle], \quad (7)$$

where $W_{lm}(i,t) = \sum_\alpha w_\alpha^i Q_{lm}(\vec{r}_\alpha,t)$ is summed over all the bond centers lying in the cell i. We restrict our attention to even-l spherical harmonics, which are invariant under inversion. The averaging over all m values ensures that the results are not affected by the choice of a particular coordinate system. Clearly, $G_l(t)$ is a measure of the ease with which a bond can execute local orientations in a given state.

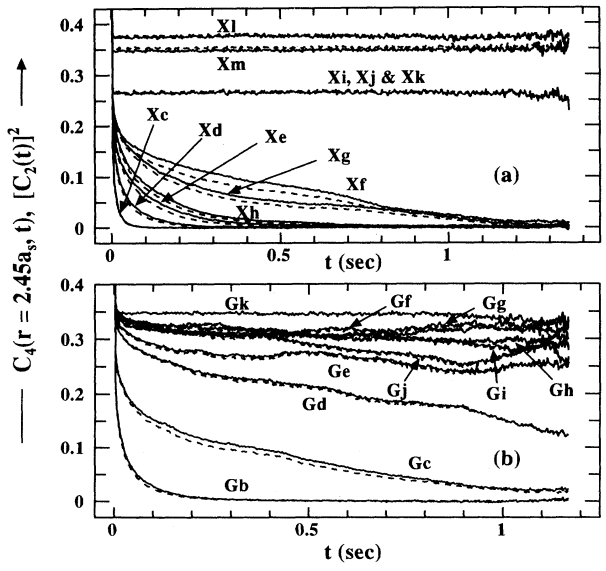

FIG. 6. Temporal growth of the four-point density correlation functions $C_4(r = 2.45a_s, t)$ (continuous lines) compared with $[C_2(t)]^2$ (dashed lines) for (a) $\phi = 0.2$ and (b) $\phi = 0.3$.

1. Quadratic rotational invariant Q_l

Figure 7 gives the results of Steinhardt *et al.* [3] for the quadratic invariants calculated for five different bond clusters, namely, (a) icosahedral (icos), (b) face-centered cubic (fcc), (c) hexagonal close pack (hcp), (d) body-centered cubic (bcc), and (e) simple cubic (sc) for $l = 2$, 4, 6, 8, and 10. Since these clusters correspond to the unit cells, identical results are valid for the infinite crystals also with these symmetries. We note that nonzero averages appear for $l \geq 4$ in hcp cluster and in cubic clusters (fcc, bcc, and sc). Also, $l = 6$ and 10 signals are nonzero for an icosahedral cluster. As calculated by Frank [4], the icosahedral packing needs $\sim 8.4\%$ less energy than fcc or hcp (the unit cluster consisting of 13 particles for all) but is not space filling.

In Fig. 8 we show the l dependence of Q_l for the final crystalline states for the runs Xm [which has the expected features as calculated for a bcc unit cell in Fig. 7(d)], Xk, and Xl. The difference between Q_i's of the Xk and the Xm and a reasonably qualitative agreement with the Xl suggest that the final crystalline state Xk has distortions present in the structure and the particles in the lattice are randomly situated, irrespective of their types. This

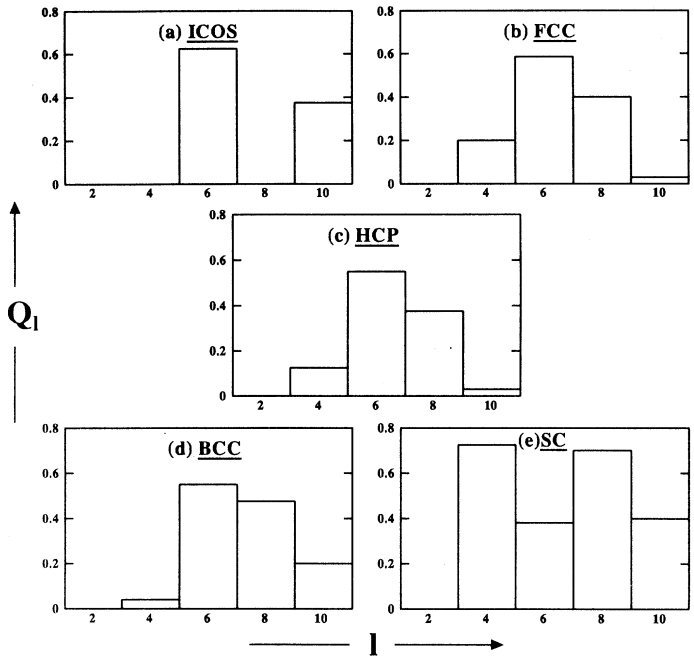

FIG. 7. Histograms of the quadratic rotational invariant Q_l for 13-atom icos, fcc, and hcp clusters, as well as for 15-atom bcc and 7-atom sc clusters. The results are taken from Ref. [2].

is in agreement with the findings [22] that the values of the internal energy E and PDF's of the final-state Xk match better with Xl than with Xm. We note that the cubic periodic boundary condition, even though it might favor the cubic order ($l = 4$) [3], is not solely responsible for the observed high value of Q_4 since it reproduces quite well the expected low value of Q_4 for the bcc unit cell [3] in the run Xm of the same system (Fig. 8). Also, the higher values of Q_6, Q_{10} and a lower value of Q_8 in the final state of the run Xk compared to Xm suggests the presence of a predominant icosahedral order in the system. In fact, comparing our results on Q_l for the CT ($\phi = 0.2$) [Figs. 9(a) and 9(b)] and the GT ($\phi = 0.3$) [Fig. 9(c)] with Fig. 7, we find that these systems show a predominant superposition of icosahedral and cubic orders. When a liquid is cooled to approach the CT, the $l = 6$ signal monotonical increases along with a nonzero $l = 10$ signal. Also, there is a sudden change in Q_l's (increase in $l \geq 4$ signals and a decrease in Q_2) at the CT, expected of a first-order phase transition. By contrast, the temperature evolution of the quadratic invariant Q_l

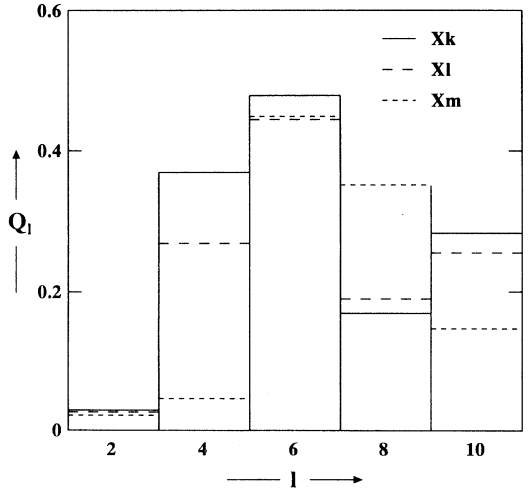

FIG. 8. Comparison of the Q_l's ($l = 2$, 4, 6, 8, and 10) for the bcc crystals obtained in the final states of the simulation runs Xk, Xl, and Xm. The temperature for all these runs is $T^* = 0.0369$.

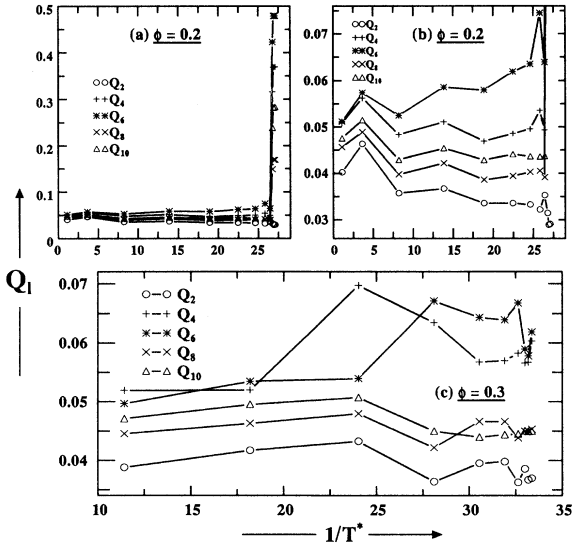

FIG. 9. Q_l versus $1/T^*$ ($l = 2$, 4, 6, 8, and 10) as a liquid is cooled to (a) and (b) $\phi = 0.2$ and (c) $\phi = 0.3$. (b) shows a blowup of the relevant portion of (a).

for the GT is entirely different. The Q_4 remain slightly higher than Q_6 in the fluid phase, but icosahedral order grows at the expense of cubic order near the T_g. The cubic order was present near the GT in the MD simulations of LJ systems [3,10].

The lower values of Q_l's in the liquid and the glassy states [Figs. 9(b) and 9(c)] as compared to their values in the corresponding perfect bond clusters (Fig. 7) is because of the averaging of these short-range orders over the entire system [10]. We note that the Q_l ($l \geq 4$) increase abruptly at the CT [Fig. 9(a) and the values in the crystal (run Xk) given in Fig. 8]. This can be due to the fact that the short-range ordered "domains" can be similarly aligned in the crystal compared to the random alignment in the liquid or glass [32]. We also note that the values of Q_l for the binary systems studied so far [7,10] are lower than that observed in the less frustrated monodisperse systems [3]. This indicates that "frustration," which is one of the characteristics of binary systems, could be an added reason for these lower values. Nevertheless the l dependence of Q_l is suntil a meaningful quantity to probe in order to gain insight about the local orientational broken symmetry.

2. *Bond-orientational autocorrelation function*

The normalized bond-orientational autocorrelation function $g_l(t) = G_l(t)/G_l(0)$ [Eq. (7)] is a very useful parameter to quantify the local orientational order and its relaxation dynamics as a function of temperature [9]. The quantities $c_2(t)$ and $g_l(t)$ together yield a sufficiently clear picture of the translational and the local bond-orientational structural relaxation of the system in a given state. Figures 2 and 3 (or Figs. 4 and 5) show the $c_2(t)$'s and $g_l(t)$'s for all l's for $\phi = 0.2$ (or $\phi = 0.3$). We see from these figures that the decay of correlation functions become slow as the liquid is cooled and is almost absent for the crystal (or the glass). The long-time saturation value of these correlation functions, which has a clear l dependence, can be taken as a measure of the nonergodicity parameter [33] used to probe the evolution of the dynamics as the liquid is cooled [34]. The l dependences of the $g_l(t)$ in the glass and in the liquid are similar to each other, implying that the orientation of the local cage surrounding a particle is similar. This is not surprising since glass is expected to be a quenched liquidlike disordered state. Contrary to this slow kinetic transition, there is an abrupt change in the l dependence of $g_l(t)$ and also in the time variation of all the correlation functions at the CT temperature T_f^* characteristic of a first-order transition. Additional interesting information gained from these figures is that both the icosahedral and cubic orders are present as seen from the dominant temporal correlations for $l = 6$ and $l = 4$ at all the temperatures. We do not understand why the uniaxial component ($l = 2$) is higher than $l = 8$ and 10 at all the temperatures (Fig. 5). The l dependence and the magnitude of the long-time saturation of $g_l(t)$'s for the final bcc crystalline states of the simulation run Xk [Fig. 3(a)] agree better with those of the run Xl [Fig. 3(b)] than with Xm (Fig. 3). This corroborates the inference that the bcc crystal in Xk has an imperfect sublattice ordering, as discussed when comparing the PDF's [22] and Q_l's for these states.

Another interesting fact about these correlation functions is that at almost all the temperatures, except for $g_6(t)$ in the crystalline state Xk, the decay of the density correlation functions is slower than the corresponding decay of the orientational functions and while cooling, the freezing of the density modes sets in at a higher temperatures compared to the orientational modes. In other words, it implies that the density fluctuations are frozen in before the orientational fluctuations.

If the system consists of short-range ordered "domains" (with similar l dependence) that are oriented at different preferred directions, $g_l(t)$ might show an l dependence different from Q_l. This is because Q_l will show the order present in the domains of the system while $g_l(t)$ will reflect the average order [32]. This, we believe, is the reason for such a difference present in our system near the GT, as seen by comparing Figs. 5 and 9(c). This is further supported by the fact that in the crystals, these domains must align with respect to each other to give rise to the identical l dependence of Q_l and $g_l(t)$, which is the case here, as seen by comparing Figs. 2, 3, 8, 9(a), and 9(b). In the case of the GT, we note that the spatial growth of such a domain to supersede the system size could also be a reason for the observed difference. Such growth is intrinsic to the spin-glass systems [16] but is not seen in the MD simulations of LJ systems [9,10] as well as in the present simulation of colloids (Fig. 6).

C. Translational and bond-orientational relaxation times

The growth of the translational and the bond-orientational relaxation times as the liquid is cooled towards the CT (Figs. 2 and 3) or the GT (Figs. 4 and 5) is well demonstrated by the corresponding correlation functions $c_2(t)$ and $g_l(t)$. One of the universal features of the relaxation dynamics near the GT is the multiexponential nature of the relaxation resulting in stretched-exponential relaxation, which is slower than single-exponential relaxation. This is often well described by the Kohlrausch-William-Watts (KWW) stretched-exponential function [35]

$$\phi(t) = \exp\left[-(t/\tau)^{\beta}\right]. \tag{8}$$

The KWW function corresponds to a continuous distribution of single-exponential decays, with a width of the distribution characterized by the exponent β, having values less than unity. The average relaxation time is given by the well-known Γ-function relation

$$\langle\tau\rangle \equiv \int_0^{\infty} \phi(t)dt = \frac{\tau}{\beta}\Gamma\left(\frac{1}{\beta}\right). \tag{9}$$

The corresponding fits with the KWW stretched-exponential functions for $c_2(t)$ and total $g_l(t)$ are also shown in Figs. 2–5 by dotted lines. The partial $g_l^{\alpha\beta}(t)$

$(\alpha, \beta = 1$ or 2) are also fitted with KWW functions with the similar accuracies and are not shown here. It is clearly seen from these figures that the correlation functions near the glass transition are better fitted by the KWW function than that for the CT. In fact, at temperatures very close to and below the GT temperature $T_g^\star$, the fits are indistinguishable from the data (whereas the fits are relatively poor as the CT is approached). The correlation functions for the crystalline states (runs Xk, Xl, and Xm) could not be fitted with the KWW functions.

The relaxation times from the correlation functions $c_2(t)$ and $g_l(t)$ over the entire temperature range of cooling towards the CT as well as the GT have been extracted with the use of Eq. (9). The "three-stage freezing" (to a crystal or a glass), noted earlier in this paper, is again confirmed from the data for relaxation times in Figs. 10 and 11. The intermediate state is clearly identified between $T_1^\star = 0.0407$ and $T_2^\star = 0.0378$ for the CT and $T_1^\star = 0.0313$ and $T_2^\star = 0.0302$ for the GT, where the system behaves relatively more liquidlike (mobile) compared to its immediate higher temperature.

It can be clearly seen in Fig. 10 that $c_2(t)$, $g_l(t)$, $g_l^{11}(t)$, and $g_l^{22}(t)$ for the liquid, before the onset of the anomalous intermediate state takes place, i.e., for $T^\star < T_1^\star$ $(= 0.0407)$ in the case of the CT, fit quite excellently to the well-known Arrhenius law

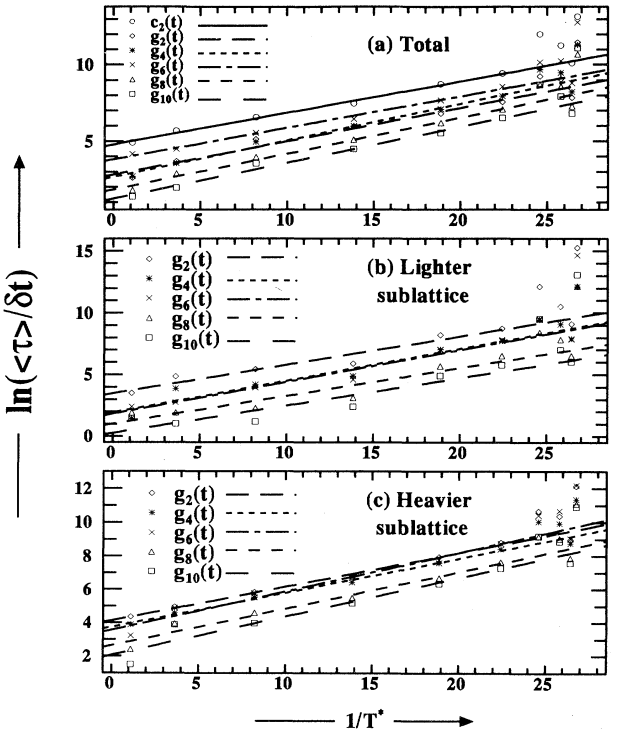

FIG. 10. $\ln\left(\frac{\langle\tau\rangle}{\delta t}\right)$ versus $1/T^\star$ for $c_2(t)$ and $g_l(t)$ ($l = 2$, 4, 6, 8, and 10) for (a) the total, (b) the lighter particles, and (c) the heavier particles at $\phi = 0.2$. The straight lines represent the fits to the Arrhenius law $\frac{\langle\tau\rangle}{\delta t} = A\exp\left(\frac{B}{T^\star}\right)$. The fit parameters are given in Table I.

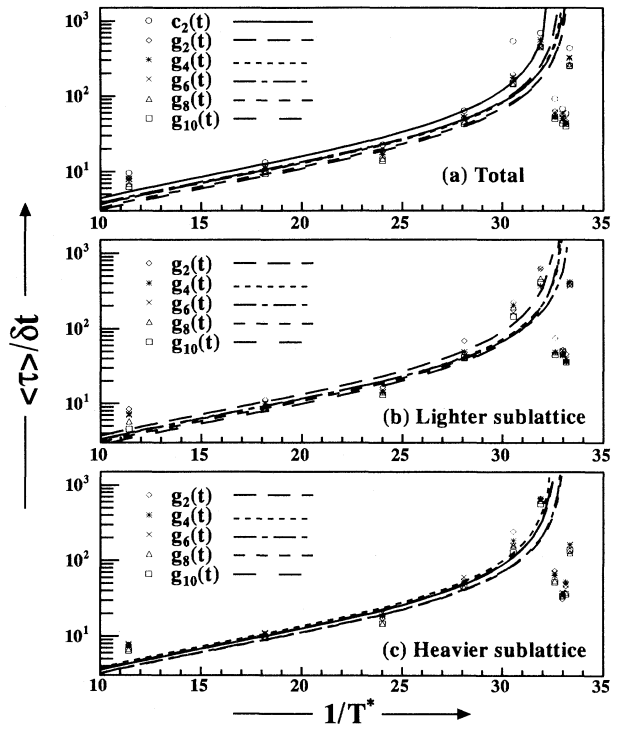

FIG. 11. Semilogarithmic plot of $\frac{\langle\tau\rangle}{\delta t}$ versus $1/T^\star$ for $c_2(t)$ and $g_l(t)$ ($l = 2, 4, 6, 8$, and 10) for (a) the total, (b) the lighter particles, and (c) the heavier particles at $\phi = 0.3$. The lines represent the fits to the VTF law $\frac{\langle\tau(T^\star)\rangle}{\delta t} = \exp\left(\frac{AT_0^\star}{T^\star - T_0^\star}\right)$. The fit parameters are given in Table I.

$$\frac{\langle\tau\rangle}{\delta t} = A\exp\left(\frac{B}{T^\star}\right), \tag{10}$$

with the fit parameters given in Table I. For the heavier particles, the translational and bond-orientational relaxation times are quite closer in magnitude to each other as compared to the same for the lighter particle. In fact, $\langle\tau\rangle$ for $l = 6$ and $c_2(t)$ happens to be nearly identical for the heavier sublattice in the entire range of temperature before the crystallization takes place.

Contrary to the above Arrhenius behavior, the increase of the relaxation times for these correlation functions with lowering the temperature is much larger near the GT, as shown in Fig. 11. This non-Arrhenius divergence of the relaxation times is much faster than the power law associated with any thermodynamic phase change (critical slowing down). The temperature dependence of $\langle\tau\rangle$ near the GT for many glass-forming liquids has been very successfully fitted to a universal functional relationship

$$\frac{\langle\tau(T^\star)\rangle}{\delta t} = \exp\left(\frac{AT_0^\star}{T^\star - T_0^\star}\right), \tag{11}$$

which is called the Vögel-Tammann-Fulcher (VTF) law [36] or, equivalently, the Williams-Landel-Ferry equation [37] in the polymer literature. Here $0 < T_0^\star < T_g^\star$. Another equivalent expression that has also been used in the literature to analyze experimental data is based on the

TABLE I. Optimal parameters for fitting the Arrhenius law [Eq. (14)] for $\phi = 0.2$ and the VTF law [Eq. (15)] for $\phi = 0.3$ to the average relaxation times $\langle\tau\rangle$. $\langle\tau\rangle$'s are extracted via Eq. (13) from the KWW [Eq. (12)] fits to $c_2(t)$ and $g_l(t)$ ($l = 2, 4, 6, 8$, and 10). The relevant fits are shown in Figs. 10 and 11, respectively.

	Total		Species 1		Species 2	
Function	A	B	A	B	A	B
	$\phi = 0.2$, Arrhenius law $\frac{\langle\tau\rangle}{\delta t} = A\exp\left(\frac{B}{T^\star}\right)$					
$c_2(t)$	4.789	0.206				
$g_2(t)$	2.812	0.218	3.486	0.231	4.131	0.203
$g_4(t)$	2.657	0.239	1.932	0.258	3.739	0.205
$g_6(t)$	3.815	0.206	1.837	0.258	3.558	0.231
$g_8(t)$	1.823	0.235	1.029	0.225	2.639	0.220
$g_{10}(t)$	1.227	0.235	0.275	0.222	2.067	0.231
Function	$T_0^\star$	A	$T_0^\star$	A	$T_0^\star$	A
	$\phi = 0.3$, VTF law $\frac{\langle\tau(T^\star)\rangle}{\delta t} = \exp\left(\frac{AT_0^\star}{T^\star - T_0^\star}\right)$					
$c_2(t)$	0.0307	10.003				
$g_2(t)$	0.0303	8.5070	0.0304	8.4895	0.0305	8.0588
$g_4(t)$	0.0301	8.5095	0.0301	7.5723	0.0305	8.3000
$g_6(t)$	0.0300	8.8815	0.0298	7.8251	0.0306	8.5925
$g_8(t)$	0.0299	7.7549	0.0302	7.0502	0.0302	7.4019
$g_{10}(t)$	0.0300	7.7267	0.0302	6.4701	0.0301	7.3639

Gaussian random energy model (GREM) used by Bässler [38] and is given by

$$\frac{\langle\tau(T^\star)\rangle}{\delta t} = \exp\left[\left(\frac{T_0^\star}{T^\star}\right)^2\right]. \tag{12}$$

There have been quite a few theoretical attempts to derive the VTF law [39] using the concept of cooperative rearranging region [40], free volume theory [41], and random energy and random coordination number model [42]. Vilgis had shown that GREM result could be obtained as a special case of the VTF form [42]. The terms "strong" and "fragile" glass-forming liquids were coined by Angell *et al.* [43] to argue the nonuniversality of the GT: on the one hand, typical strong glass formers (network materials such as various oxide glasses) show an Arrhenius temperature dependence of $\langle\tau\rangle$, whereas, on the other hand, the fragile (non-network molecular or ionic) glass-forming liquids with large fluctuating coordination numbers show a non-Arrhenius increase in $\langle\tau\rangle$ with decreasing temperature. It has been pointed out [17] that it is possible to obtain both of these apparently opposite features from the VTF law, depending on the "strength" of the glass former as reflected by the value of the parameter A in Eq. (11), which may vary from about 3 to 100. The smaller the value of A, the more fragile the glass former [44].

Our data are fitted better by the VTF law than by the GREM equation, in agreement with the similar findings for the ergodicity-diffusion parameters for the soft-sphere systems (interacting via the r^{-12} potential) and the ergodicity and the self-diffusion parameters for the LJ systems [45]. In Ref. [45], the self-diffusion coefficient had shown an Arrhenius behavior for the soft-sphere mixtures in contrast to the non-Arrhenius VTF behavior seen for the LJ systems. It was argued to be due to the lack of short-range cooperativeness (e.g., icosahedral order, etc.) in the soft-sphere systems in contrast to the LJ systems. Our simulations clearly oppose this conjecture. In fact, like in the LJ systems, short-range bond-orientational order (e.g., icosahedral, cubic, etc.) as well as very strong cooperative behaviors (e.g., jump diffusion, etc.) [23] do prevail near the GT in the soft-sphere systems as well.

In Fig. 11 we have shown the VTF fits for the temperature dependence of the total $\langle\tau\rangle$, extracted from these correlation functions, along with those for lighter and heavier sublattices. Table I gives the relevant fitting parameters. The values of the "ideal" GT temperature $T_0^\star$ obtained from the fits of $c_2(t)$ and different $g_l(t)$ are very close to each other. Our data show that the material-dependent phenomenological strength parameter A is not very sensitive to the type of the physical quantity being probed. Its value lies approximately between 7 and 8.5 for the orientational correlations and is about 10 for the translational one. This indicates that the colloidal suspensions are extremely fragile glass formers in the notation of Angell *et al.* [43], where the rapid decrease of the relaxation time as the temperature increases is associated with the multiplicity of configurations of the ground states. The drastic effects shown in the GT and the possibility of getting quite close to $T_g^\star$ [17] are the essential features that make fragile systems of considerable importance.

The use of mode-coupling theories (MCT's), devised originally to describe the microscopic dynamics of dense liquids, has made significant advancements possible in the understanding of the dynamical behavior of supercooled liquid near the GT. The basic version of the theory due to Bengtzelius *et al.* and developed independently by Leutheusser [46] and further by Götze and Sjögren [47] incorporates explicitly the delayed nonlinear coupling between density fluctuations and makes detailed predictions regarding the relaxation dynamics near the GT. One of

the predictions of the MCT [47] for the GT is the time-temperature superposition principle: as $T^\star$ approaches some critical temperature $T_c^\star$ from above, the "shape" of any given correlation function does not depend on the temperature, in the α relaxation regime. This would imply a "constant" stretching exponent β of Eq. (8) over this range of temperature. By properly scaling the time, the correlation functions at various temperatures would then fall on a unique "master curve," which is often well fitted by a simple KWW stretched-exponential function. Experiments [48,44] and simulations [e.g., Ref. [49] and our results for the Van Hove self-correlation function $F_\alpha^s(q,t)$ [30]] have provided evidence in support of this scaling property. By contrast, experimental evidence for a strong temperature dependence of β also exists for a variety of glass formers (for example, see the references cited in the Ref. [44]). Our data for β show a striking linear dependence of $1/T^\star$ [Fig. 12(b)] for all the correlation functions studied here when approaching $T_g^\star$ from above. On the contrary, β is more or less temperature independent in the liquid phase, well above the crystallization [Fig. 12(a)]. The shape of different correlation functions, as reflected from the values of the Kohlrausch stretching exponent β, tends to become almost identical (approximately 0.05) near the GT, in contrast to the case of the CT, where β seems to fluctuate about a constant value. We note that at high temperatures, since the correlation functions decay to zero very fast, there are not enough data points for the β of the fitted curve of Eq. (8) to be reliable. Hence β values for those $T^\star$ are omitted from Fig. 12. Though these correlation functions fail to show the time-temperature superposition principle, we have confirmed that [30] it is clearly valid for the self-intermediate scattering functions $F(q,t)$. This is not entirely unexpected for $g_l(t)$, since these functions measure a different property than $F(q,t)$ and α relaxation is known to depend on the quantity considered. The reason for the difference in results between $c_2(t)$ and $F(q,t)$ could be twofold. First, the MCT predictions are meant for the density autocorrelators of the type $F(q,t)$, for fixed values of wave vectors q, whereas, because of dividing the simulation box in grids and then defining a "lattice-gas" variable $n(i,t)$, the correlation functions, e.g., $c_2(t)$, defined by this variable become extremely coarse grained and dependent on the uniformity of the meshing. Second, the closest approximation of $F(q,t)$ should, in principle, be the Fourier transform of $C_4(r,t)$ (the one to one correspondence of the two functions are yet to be checked for), but what we have measured is $c_2(t)$, where the q dependence is not incorporated. Apart from the experimental findings [50] and the theoretical inference [51] that fragile glass formers are prone to show a strong temperature dependence, it was also suggested [43,52] that there could be a connection between the non-Arrhenius form [Eq. (11)] and the nonexponentiality [Eq. (8)]. This was strengthened by the previous findings [50] that the more fragile the system (i.e., the lower the value of A), the steeper the approach towards the stretched relaxation ($\beta \simeq 0$) as a function of temperature. This is not the case in Fig. 12(b), where $A \sim 10$ for $c_2(t)$ and $A \sim 8$ for $g_l(t)$. Thus our results, i.e., the approach towards $\beta \simeq 0$ slows down with lowering A, question the suggestion of a general relationship between the nonexponential nature of the correlation functions and non-Arrhenius behavior of the relaxation times.

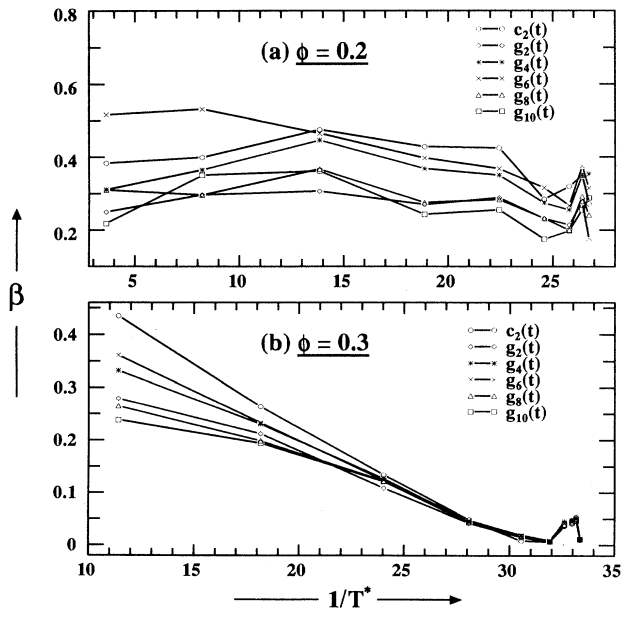

FIG. 12. Exponent β obtained from the stretched-exponential [Eq. (8)] fits to $c_2(t)$ and total $g_l(t)$ ($l = 2, 4, 6, 8$, and 10) plotted versus $1/T^\star$ for (a) $\phi = 0.2$ and (b) $\phi = 0.3$.

III. SUMMARY AND CONCLUSIONS

In this paper we have reported the BD results on the translational and bond angle correlation functions for a simple Derjaguin-Landau-Vernay-Overbeek model of the binary polyball mixture, as it is cooled towards forming a crystal or a glass. The static parameters and the mean-squared displacement of the same states are reported in paper I [22]. The main results and conclusions of this paper are as follows.

(i) We quantify the translational order in terms of the two-point normalized $c_2(t)$ and four-point $C_4(r,t)$ density autocorrelation functions. The nearest-neighbor orientational order is quantified in terms of the l-dependent quadratic rotational invariant Q_l and the normalized bond-orientational autocorrelation functions $g_l(t)$.

(ii) The value of $C_4(r,t)$ being nearly equal to $[C_2(t)]^2$ for $r > 2a_s$ at all temperatures when a liquid is quenched to a metastable glass shows that there is no correlation length in the system, which is diverging near the glass transition. On the other hand, the difference between these two quantities increases as the crystal transition is approached and eventually goes to zero in the crystal state of the system, indicating that there is a finite growth of correlation length as a liquid is cooled towards a crystal.

(iii) The l dependence of Q_l in the crystalline state ($\phi = 0.2$) does not match that of a perfect bcc lattice

(with simple-cubic sublattice ordering). This suggests that the crystalline state, whose $g(r)$ shows bcc order (paper I [22]), has distortions present in its structure. The changes of the descending order of magnitude from $Q_4, Q_6, Q_{10}, Q_8, Q_2$ in the liquid to $Q_6, Q_4, Q_8, Q_{10}, Q_2$ in the glass and $Q_6, Q_4, Q_{10}, Q_8, Q_2$ in the crystal indicate that icosahedral ($l = 6$) order predominates at the cost of cubic order ($l = 4$) near the glass transition as well as the crystal transition.

(iv) The normalized $c_2(t)$ decays slower than $g_l(t)$ as a liquid is cooled either towards a crystalline or a glassy state. These correlation functions for a supercooled liquid freezing towards a glass fit well to the KWW stretched-exponential form $\exp\left[-(t/\tau)^{\beta}\right]$, supporting the existing notion that stretching or multirelaxation processes could be a universal feature of the dynamics near glass transitions.

(v) The average translational and bond-orientational relaxation times $[\langle\tau\rangle = \frac{\tau}{\beta}\Gamma(\frac{1}{\beta})]$ are extracted from the fitted stretched-exponential functions as a function of $T^{\star}$. The temperature dependence of $\langle\tau\rangle$ is Arrhenius $([\langle\tau(T^{\star})\rangle/\delta t] \propto \exp(B/T^{\star}))$ for a liquid to crystal transition while it can be approximated reasonably well by the VTF law $([\langle\tau(T^{\star})\rangle/\delta t] = \exp[AT_0^{\star}/(T^{\star} - T_0^{\star})])$ for a liquid to glass transition. The value of the parameter A points out that the colloidal suspensions are fragile glass formers such as the organic and molecular liquids. The GREM fails to explain the temperature dependence of $\langle\tau\rangle$.

ACKNOWLEDGMENTS

We thank the Indo-French Centre for the Promotion of Advanced Research (Project No. 607.1) for financial support. We made use of the computational resources of the Jawaharlal Nehru Center for the Advanced Scientific Research, India and the Supercomputer and Educational Research Center of the Indian Institute of Science, India. We thank Professor Chandan Dasgupta for the program to calculate the correlation functions and Professor Jayant Banawar for useful discussions. S.S. acknowledges useful discussions with Siddhartha Shankar Ghosh, Jaydeb Chakrabarti, and A. V. Indrani at various stages of the work.

[1] For a recent collection of reviews, see *Bond-Orientational Order in Condensed Matter Systems*, edited by K. J. Strandburg (Springer-Verlag, New York, 1992).
[2] D. R. Nelson and J. Toner, Phys. Rev. B **24**, 363 (1981).
[3] P. J. Steinhardt, D. R. Nelson, and M. Ronchetti, Phys. Rev. Lett. **47**, 1297 (1981); Phys. Rev. B **28**, 784 (1983).
[4] F. C. Frank, Proc. R. Soc. London Ser. A **215**, 43 (1952).
[5] D. R. Nelson, Phys. Rev. Lett. **50**, 982 (1983); Phys. Rev. B **28**, 5515 (1983); D. R. Nelson and M. Widom, Nucl. Phys. B **240**, 113 (1984).
[6] S. Sachdev and D. R. Nelson, Phys. Rev. Lett. **53**, 1947 (1984); Phys. Rev. B **32**, 1480 (1985); S. Sachdev, *ibid.* **33**, 6395 (1986); S. Sachdev, in *Bond-Orientational Order in Condensed Matter Systems* (Ref. 1), p. 255.
[7] R. D. Mountain and D. Thirumalai, Phys. Rev. A **36**, 3300 (1987); D. Thirumalai and R. D. Mountain, J. Phys. C **20**, L399 (1987).
[8] J. G. Amar and R. D. Mountain, J. Chem. Phys. **86**, 2236 (1987).
[9] C. Dasgupta, A. V. Indrani, S. Ramaswamy, and M. K. Phani, Europhys. Lett. **15**, 307 (1991).
[10] R. M. Ernst, S. R. Nagel, and G. S. Grest, Phys. Rev. B **43**, 8070 (1991).
[11] R. D. Mountain and A. C. Brown, J. Chem. Phys. **80**, 2730 (1984).
[12] J. S. van Duijneveldt and D. Frenkel, J. Chem. Phys. **96**, 4655 (1992).
[13] F. H. Stillinger and R. A. LaViolette, Phys. Rev. A **34**, 5136 (1986).
[14] H. Jónsson and H. C. Andersen, Phys. Rev. Lett. **60**, 2295 (1988).
[15] A. Clarke and H. Jónsson, Phys. Rev. E **47**, 3975 (1993).
[16] K. Binder and A. P. Young, Rev. Mod. Phys. **58**, 881 (1986).
[17] J. P. Sethna, Europhys. Lett. **6**, 529 (1988).
[18] M. Cohen and G. Grest, Phys. Rev. B **20**, 1077 (1979); E. Donth, in *Glasübergang* (Akademie-Verlag, Berlin, 1981); Acta Polym. **30**, 481 (1979); J. Non-Cryst. Solids **131-133**, 204 (1991); **53**, 325 (1982); W. Kauzmann, Chem. Rev. **43**, 219 (1984); D. L. Stein and R. G. Palmer, Phys. Rev. B **38**, 12 035 (1988); J. H. Gibbs and E. A. DiMarzio, J. Chem. Phys. **28**, 373 (1988); T. R. Kirkpatrik, D. Thirumalai, and P. G. Wolynes, Phys. Rev. A **40**, 1045 (1989).
[19] P. K. Dixon, L. Wu, S. R. Nagel, B. D. Williams, and J. P. Carini, Phys. Rev. Lett. **65**, 1108 (1990); L. Wu, P. K. Dixon, S. R. Nagel, B. D. Williams, and J. P. Carini, J. Non-Cryst. Solids **131**, 32 (1991); N. Menon, K. P. O'Brien, P. K. Dixon, L. Wu, S. R. Nagel, B. D. Williams, and J. P. Carini, *ibid.* **141**, 61 (1991); L. Wu, Phys. Rev. B **43**, 9906 (1991); N. Menon, S. R. Nagel, and D. C. Verenus (unpublished).
[20] E. W. Ficher, E. Donth, and W. Steffen, Phys. Rev. Lett. **68**, 2344 (1992); N. Menon and S. R. Nagel (unpublished).
[21] For a review, see A. K. Sood, in *Solid State Physics*, edited by H. Ehrenreich and D. Turnbull (Academic, New York, 1991), Vol. 45, p. 1.
[22] S. Sanyal and A. K. Sood, preceding paper, Phys. Rev. E **52**, 4154 (1995).
[23] S. Sanyal and A. K. Sood (unpublished).
[24] H. M. Lindsay and P. M. Chaikin, J. Chem. Phys. **76**, 3774 (1982).
[25] R. O. Rosenberg, D. Thirumalai, and R. D. Mountain, J. Phys. Condens. Matter **1**, 2109 (1989).
[26] R. O. Rosenberg and D. Thirumalai, Phys. Rev. A **36**, 5690 (1987).
[27] D. L. Ermak and Y. Yeh, Chem. Phys. Lett. **24**, 243 (1974); D. L. Ermak, J. Chem. Phys. **62**, 4189 (1975); **62**, 4197 (1975); D. L. Ermak and J. A. McCammon, *ibid.* **69**, 1352 (1978).
[28] D. L. Ermak and Y. Yeh, Chem. Phys. Lett. **24**, 243

(1974).
[29] M. P. Allen and D. J. Tildesley, *Computer Simulation of Liquids* (Oxford University Press, London, 1987).
[30] S. Sanyal, Ph.D. thesis, Indian Institute of Science, 1994 (unpublished).
[31] M. Hoare, Ann. N. Y. Acad. Sci. **279**, 186 (1976).
[32] Chandan Dasgupta (private communication).
[33] S. F. Edwards and P. W. Anderson, J. Phys. F **5**, 965 (1975).
[34] W. van Megen and P. N. Pusey, Phys. Rev. A **43**, 5429 (1991); W. van Megen, S. M. Underwood, and P. N. Pusey, Phys. Rev. Lett. **67**, 1586 (1991); W. van Megen and S. M. Underwood, Phys. Rev. E **47**, 248 (1993).
[35] G. Williams and D. C. Watts, Trans. Faraday Soc. **66**, 80 (1970).
[36] H. Vögel, Z. Phys. **22**, 645 (1921); G. S. Fulcher, J. Am. Ceram. Soc. **8**, 339 (1925); G. Tammann and W. Hesse, Z. Anorg. Allgem. Chem. **156**, 245 (1926).
[37] M. L. Williams, R. F. Lendel, and J. D. Ferry, J. Am. Chem. Soc. **77**, 3701 (1955); J. D. Ferry, *Viscoelastic Properties of Polymers* (Wiley, New York, 1980).
[38] H. Bässler, Phys. Rev. Lett. **58**, 767 (1987).
[39] P. W. Anderson, in *Ill Condensed Matter*, edited by R. Balian *et al.* (North-Holland, Amsterdam, 1979).
[40] G. Adam and J. H. Gibbs, J. Chem. Phys. **43**, 139 (1965).
[41] M. H. Cohen and D. Turnbull, J. Chem. Phys. **31**, 1164 (1959); **34**, 120 (1961); **52**, 3038 (1970); Nature (London) **203**, 964 (1964); D. Turnbull, J. Phys. (Paris) Colloq. **35**, C4-1 (1974); M. Cohen and G. Grest, Phys. Rev. B **20**, 1077 (1979); G. Grest and M. H. Cohen, Adv. Chem. Phys. **48**, 455 (1981); D. Turnbull and M. Cohen, J. Chem. Phys. **34**, 120 (1961).
[42] T. A. Vilgis, J. Phys. Condens. Matter **2**, 3667 (1990); Phys. Rev. B **47**, 2882 (1993).
[43] C. A. Angell, A. Dworkin, P. Figuiere, A. Fuchs, and H. Szwarc, J. Chem. Phys. **82**, 773 (1985); J. Phys. Chem. Solids **49**, 863 (1988); J. Non-Cryst. Solids **191**, 13 (1991).
[44] L. Bröjesson, M. Elmroth, and L. M. Torell, Chem. Phys. **149**, 209 (1990).
[45] R. D. Mountain and D. Thirumalai (unpublished); Phys. Rev. E **47**, 479 (1993).
[46] U. Bengtzelius, W. Götze, and A. Sjölander, J. Phys. C **17**, 5915 (1984); U. Bengtzelius, Phys. Rev. A **34**, 5059 (1986); **33**, 3433 (1986); E. Leutheusser, *ibid.* **29**, 2765 (1984).
[47] For reviews on MCT, see W. Götze, in *Liquids, Freezing and the Glass Transition*, Proceedings of the Les Houches Summer School of Theoretical Physics, Session L1, edited by J. P. Hansen, D. Levesque, and J. Zinn-Justin (North-Holland, Amsterdam, 1991), p. 287; W. Götze and L. Sjögren, Rep. Prog. Phys. **55**, 241 (1992).
[48] F. Mezei, W. Knaak, and B. Farago, Phys. Rev. Lett. **58**, 571 (1978); **54**, 571 (1987); Phys. Scr. **T19**, 363 (1987); W. Knaak, F. Mezei, and B. Farago, Europhys. Lett. **7**, 529 (1988).
[49] G. Pastore, B. Bernu, J. P. Hansen, and Y. Hiwatari, Phys. Rev. A **38**, 454 (1988).
[50] G. Grimsditch and L. M. Torell, in *Dynamics of Disordered Materials*, edited by D. Ritcher, A. H. Dianoux, W. Pretry, and H. Teixeira (Springer, Berlin, 1989).
[51] K. L. Ngai, J. Non-Cryst. Solids **131-133**, 80 (1991), and references cited therein.
[52] G. McDuffie and T. A. Litovitz, J. Chem. Phys. **37**, 1699 (1962).